

GC-MS, DFT, LOL, ELF, NCI-RDG, kinetic energy, reactivity, stability, topological molecular descriptors evaluation on 2-propanone, 1-hydroxy-, Isopropyl alcohol and Glycerin: For NLO application

E Dhanalakshmi^{1*}, P Rajesh², M Anbarasu³, P Kandan⁴, A Raaza⁵ & M Prabhakaran⁶

¹Department of Physics and Department of Education; ²Department of Physics; School of Basic Science; ³Department of Agronomy, School of Agriculture; & ⁵Research and Development, Vels Institute of Science, Technology & Advanced Studies (VISTAS), Pallavaram, Chennai-600 117, Tamil Nadu, India

⁴PG and Research Department of Mathematics, Government Arts College, Chidambaram, Annamalai University, Annamalai Nagar-608 002, Tamil Nadu, India

⁶Department of Physics, Saveetha School of Engineering, Saveetha Institute of Medical and Technical Sciences (SIMATS), Chennai-602 105, Tamil Nadu, India

Received 12 December 2024; revised 30 January 2025

The present article provides spectroscopic technique gas chromatography-mass spectrometry (GC-MS) and density functional theory (DFT) analysis to the examined molecular structure of these three compounds namely 2-Propanone, 1-hydroxy-, Isopropyl alcohol and glycerin synthesis from *Hybanthus enneaspermus* plant by using green method. The optimized structure of title compounds is obtained by using a hybrid DFT/B3LYP/6-311++G(d, p) approach for stability prediction. Molecular descriptors of natural bond orbital (NBO), highest orbital molecular orbital (HOMO), lowest unoccupied molecular orbital (LUMO), global reactivity, and Mulliken charge to determine its structural characterization, chemical stability and biological aspects interpreted by the same set. Localized orbital locator (LOL), electron localized function (ELF) has been investigated to understand the localization and delocalization of three molecules. The strong, weak and van der Waals interactions can identify based on electron density and were estimated by reduced density gradient (RDG) analysis. The thermodynamic properties of entropy (S), capacity (V) and specific heat have been estimated. The dipole moment (μ) and polarizability (α) have been calculated to predict the nature of 2-propanone, 1-hydroxy- (2PH), isopropyl alcohol (IA) and glycerin (GL) molecules and showed excellent nonlinear optical (NLO) candidates. Moreover, the qualitative structure-activity relationship/qualitative structure-property relationship QSAR/QSPR analysis topological descriptors have a strong correlation with physical properties, which is ideally suitable for drug discovery used to prevent enormous biological activity.

Keywords: DFT, GC-MS, NLO, Thermodynamic Properties, Topological indices

The 2-propanone, 1-hydroxy- is also called hydroxyacetone, isopropyl alcohol and glycerine; these compounds are naturally synthesized from the medicinal plant of *Hybanthus enneaspermus*. Those molecules contain carbonyl, hydroxyl, methyl and methylene groups it's used to make imidazole compounds for high blood pressure, heart and kidney failure medicines¹. The aldehyde, keto and enediol forms of 2PH (acetol) were identified to have unique infrared absorption bands. These bonds were then utilized to investigate the effects of temperature, acid/base catalysis, and solvent on the enolization reactions². The 1-pyrrolines, 2-oxopropanal, and hydroxy-2-propanone, those compounds are

significant agents in the production of food flavor³. In certain situations, reducing nausea with inhalation of isopropyl alcohol requires putting a sterile pad beneath the nose. The semiconductor sector wants to eliminate tiny particles from IA, which is frequently employed to clean fine patterns in IA is desired in the industry⁴. The computational analysis and the binary interaction location have been stimulated by isopropyl alcohol⁵. The glycerine drug is employed as a moisturizer, to treat and avoid rough, scaly, itchy, dry skin as well as mild allergic reactions (such as rash from diapers and burns to the skin from radiotherapy). Glycerin is reported to function in cosmetics as a denaturant, fragrance ingredient, hair conditioning agent, humectant, oral care agent, oral health-care drug, skin protectant, skin conditioning agent humectant, and viscosity-decreasing agent⁶. The above-discussed

*Correspondence:
E-mail: jdkrishii2015@gmail.com

application has encouraged develop recharge on 2PH, IA and GL components. The goal of the current study is to describe the green synthesis method that can be applied for size reduction, cost-effective, rapid and density functional theory is eco-friendly to calculate three compounds which used a wide range of applications in this field on pharmaceutical industry and modern system. Quantum chemical calculation exploration is one of the most helpful methods to exhibit research tools for modelling drugs, biological compounds and products to identify the structural energy values, molecular stability and designing of drugs. The geometrical parameter, Fermi energy and the frontier molecular orbitals are important parameters that can be used to predict the strength and stability and global reactivity descriptors provide structural information of 2PH, IA and GL compounds obtained by DFT/B3LYP/6-311++G(d, p) level, which play an important role in biological reactions. The natural bond orbital (NBO) analysis examined the intermolecular interaction and highest bond strength across the donor and acceptor. Topological analysis of localized orbital locator (LOL), electron localized function (ELF) and reduced density gradient (RDG) has been executed by the Multiwfn3.7 approach. Thermodynamic properties of entropy, capacity and specific heat capacity are evaluated by Perl-Script. The nonlinear optical (NLO) properties of polarizability and dipole-moment of 2PH, IA and GL compounds have been performed. The ten degree-based topological indices correlated with physical characteristics of boiling point ($^{\circ}\text{C}$), melting point, molar refractivity (cm^3), polarity (cm^3), polar surfaces area (\AA^2) and complexity of components successively^{7,8}.

Materials and Methods

Extraction of bioactive components

The fresh plants of *Hybanthus enneaspermus* were plucked, the collected 2 kg and were brought to the laboratory for further investigation. The gathered plant was properly cleaned with running water to get rid of any remaining dust and then the plant parts were cut into smaller pieces for fast drying at room temperature⁹⁻¹¹. The plant material reached after drying was crushed into fine powder with the help of an electric grinder and that powder dip with ethanol 2:1 ratio at 48h after using Whatman quality 41 quick ash less filtration paper, 110 mm round to filtered extract to run soxhlet apparatus widely used to extract

valuable bioactive components (crude) and stored in airtight containers at room temperature for further analysis.

GC-MS analysis

The gas chromatography-mass spectrometry (GC-MS) analysis identifies bio-components from plant extract thus, GC separates chemical compounds from a mixture of samples and the MS technique is used to measure molecular weight, chemical structure and retention time. That result was reported from GC-MS in three-dimensional distributed mass spectra used to confirm the structure and identify unknown compounds^{12,13}. In the current investigation, GC-MS was carried out using Shimadzu-QP2010 plus and starting column temperature 1000–2800 $^{\circ}\text{C}$ the temperature were balanced for 5 min, the mass spectrometry scan range 45-450 (MHz) and the ethanol extract of *Hybanthus enneaspermus* sample of total running time at 25 min that obtained mass spectra were compared with database stored in national institute of standard and technology (NIST) mass spectral library.

Topological indices descriptions

The amount of work required of pharmaceutical and chemical investigators increased dramatically when they had to conduct numerous chemical experiments to determine the pharmaceutical, chemical in nature and biological properties of novel components. But the medicines, despite great progress in the area of mathematical drug development. Finding and optimizing the lead molecules quickly and affordably continues to be a crucial phase in the drug discovery process. Over the past ten years, the theoretical tool approaches have developed at a quick pace, which has contributed significantly to the creation of several medications that are currently on the market or undergoing clinical trials¹⁴. These computational tool techniques are based on the use of a virtual world of computer-generated hypotheses, which are tested for practicality. Several computational device approaches depend on the application generated by computed assumptions in the virtual world that are validated for effectiveness. Without utilizing a weight laboratory, forecast the characteristics of medicine by examining its molecular structure and applying popular chemical graph mathematical method known as the topological indices, also called the molecular descriptors¹⁵. The topological indicators are numerical values

connected to biochemical structure that are employed to correlate molecular structure with a variety of attributes, including physical attributes, pharmacological activity and chemical reactant behavior¹⁶. To determine topological indicators, the drug structure can be visualized chemical graph, with each vertex denoting a single atom and every edge denoting the chemical connection among the atoms¹⁷.

Computational details

The computational estimation of PH, IA and GL compounds has been performed by applying the Gaussian 09 software using B3LYP/6-311++G(d, p) set. The B3LYP demonstrates the Lee-Yang-Parr, which considers cost-effective techniques¹⁸. Determining the basic vibrational characteristic of the optimized molecular and electronic structure of the components can be improved by execution DFT technique¹⁹. The Gauss View 06W package has been used to display molecular electrostatic potential (MEP) diagram as well as HOMO and LUMO areas²⁰. The NBO is used to estimate delocalization or hyper-conjugation within the second-order perturbation approach²¹. Topological analysis of LOL, ELF, ESP and RDG were used to verify non-covalent interaction interpreted by multi-functional wave function (Multiwfn) and visual molecular dynamics (VMD) softwares^{22,23}. Thermodynamic in perl (THERMO.PL) script tool used to determine thermodynamics parameters with Gaussian output data²⁴. The docking investigation exhibits ligand-protein interaction was used to execute Autodock 4.2.6 and Python 3.8.2 software. The Avogadro and molecular graphics dynamics (MGL) Tool 1.5.6 have been used to express optimization of ligands as well as visualization of the molecular structure²⁵.

Result and Discussion

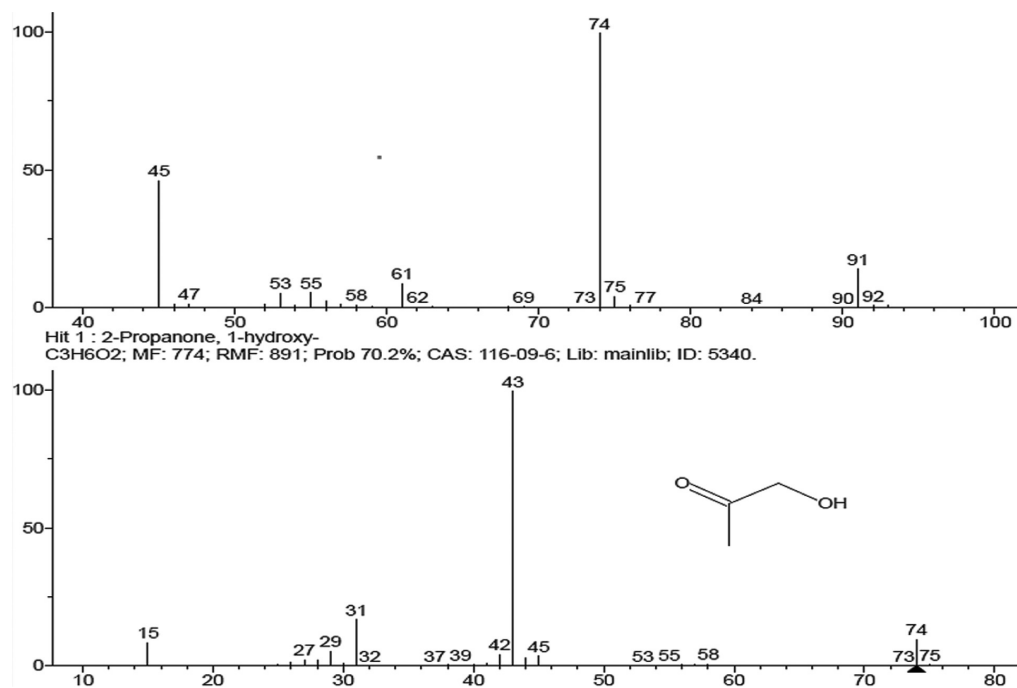
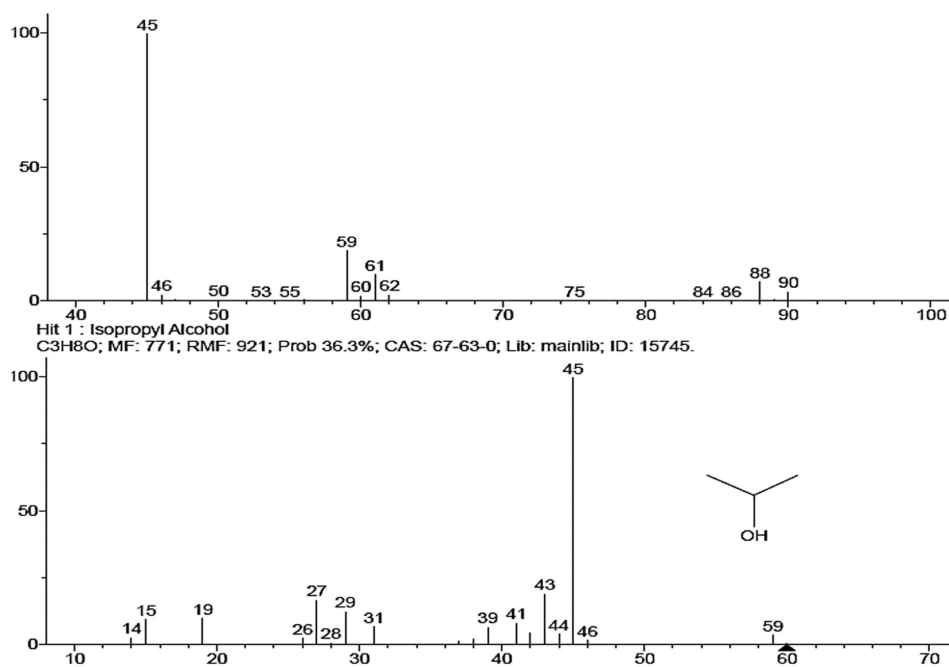
GC-MS investigation extracts of *Hybanthus enneaspermus*

The GC-MS can support traditional and industrial applications as a natural remedy. Furthermore, it also helps in determining the best techniques for collecting these substances, which data will be presented in the environment of their potential biological or therapeutic significance. The GC-MS chromatogram investigated the carbinol extract of *Hybanthus enneaspermus* and reported multiple major components. The MS fingerprint of bio-components can be conformed to molecular structure from the NIST data library that has over 62000 patterns. The

evaluation of individual constituent part was identified by molecular name, weight and structure²⁶. The corresponding percentage quality of each compound has been estimated by correlating the maximum peak region to the total region²⁷. In the present investigation the following three components 2PH, IA and GL are identified from GC-MS results as displayed in (Figs. 1-3). The GC-MS results of 2PH, IA and GL components have been identified based on the molecular formula ($C_3H_6O_2$, C_3H_8O and $C_3H_8O_3$), molecular weight (74.0, 60.1 and 15.6 g/mol) and retention time (12.15, 14.26 and 15.6 min), which database compared with NIST database library are summarized in (Table 1). Furthermore, we have performed DFT, thermodynamic properties, and NLO, topological indices by using 2PH, IA and GL components after conformation from GC-MS analysis, respectively.

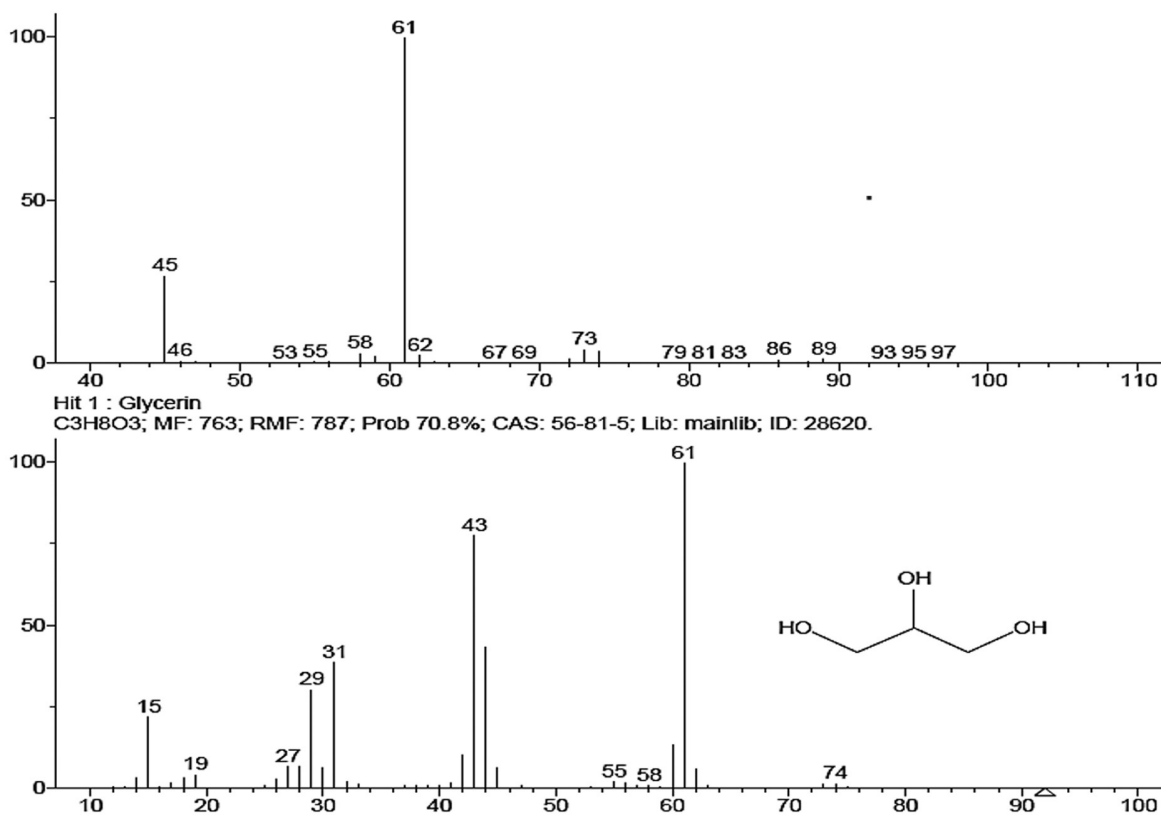
Molecular parameters energy values on 2PH, IA and GL compounds

The theoretical approach of bond angle and bond length used to predict the physical and chemical properties, molecular shape, chemical reactivity and stability, and repulsion between the electron pairs in the valence shell were determined by the geometry of molecules. In the current research, the three molecular properties of bond angle and bond length, Mulliken atomic charge, NBO analysis, global reactivity descriptors like electronegativity, chemical hardness and softness described by B3LYP/6-311++G(d, p)²⁸ approach are mentioned in (Table 2). The bond angle decreases, the central atom contains more polarizable and the bond angle increases, the outer atoms represent more polarization in the 3 dimensional molecular geometry provided by Debye polarizability model^{29,30}. The title molecules contain higher bond angle 2PH=($C_1-C_2-O_4$) \rightarrow 122.60, IA=($C_2-C_1-C_3$) \rightarrow 112.52 and GL=($O_1-C_2-H_8$) \rightarrow 111.86° and lower bond length 2PH=($C_2-C_1-H_7$) \rightarrow 107.08, IA=($C_2-C_1-O_4$) \rightarrow 106.24 and GL=($C_3-O_4-H_{11}$) \rightarrow 105.11°. The above bond angles of polarizability increased which is directly proportional to dispersive force and having higher covalent character become more strongly. If the dispersive force gets stronger between the bond angles it's to be attached to their neighbours atoms strongly and increasing polarizability. Furthermore, the bond length used to calculate the different covalent bonds determined by single, double and triple bonds. The small bond length becomes the stronger force of attraction between the bonded atoms

Fig. 1 — 2-Propanone, 1-hydroxy- compound separate from *Hybanthus enneaspermus*Fig. 2 — Isopropyl alcohol compound separate from *Hybanthus enneaspermus*

than the longer bond length represents looser attraction between the atoms. In this paper, the three molecules demonstrate the small bond distance $2PH=(O_5-H_{11}) \rightarrow 0.96$, $IA=(O_4-H_{12}) \rightarrow 0.96$ and $GL=(O_6-H_{14}) \rightarrow 0.96$ Å are strong attraction it's required more energy to break the bonds greater than $2PH=(C_1-C_2) \rightarrow 1.52$, $IA=(C1-C2) \rightarrow 1.52$ and

$GL=(C_3-C_5) \rightarrow 1.52$ Å are less attraction its required minimum energy to break the bonds, respectively. The Mullikan atomic charge describes how the molecules gain or lose electrons in the direction of positive and negative charge among the chemical bonding. Their value indicates a strong correlation with the strength of the bond formed across

Fig. 3 — Glycerin compound isolate from *Hybanthus enneaspermus*Table 1 — Report on bioactive compounds from *Hybanthus enneaspermus*

Name of the Compound	Molecular Formula	Molecular weight (g/mol)	Retention time (min)
2-Propanone, 1-hydroxy-	C ₃ H ₆ O ₂	74.0	12.15
Isopropyl Alcohol	C ₃ H ₈ O	60.1	14.26
Glycerin	C ₃ H ₈ O ₃	92.0	15.36

the individual atom in three-dimensional ways^{31,32}. Mulliken charges estimated on the three compounds, which indices highest negative charge and electrophilic attack occupy around hydrogen atoms $H_{11} \rightarrow 0.306$ (2PH), $H_{12} \rightarrow 0.298$ (IA) and $H_{14} \rightarrow 0.304$ (GL) a.u., these negative growth rates represent population decreases (donor) whereas highest positive charge and nucleophilic attack occupies nearby oxygen atoms $O_1 \rightarrow -0.506$ (2PH), $O_4 \rightarrow -0.526$ (IA) and $O_1 \rightarrow -0.526$ (GL) a.u. these positive growth rate represent population increases (acceptor) which play important role in chemical reactivity of the title molecules.

The number of molecular parameters, such as the electronic transition of energy level, HOMO, LUMO, electron charge transfer (ΔN_{\max}), ionization potential (IP), electron affinity (EA), and global descriptors are used to conclude energy gap values for chemical stability and reactivity. The stronger polarizable

compound exhibiting lower kinetic stability but excellent chemical reactivity is one with a shorter energy gap. The HOMO, LUMO minimum energy gap report easy transition, high reactivity and low stability and the maximum energy gap relate to harder transition, low reactivity and high stability. In this present investigation describes three components 2PH, IA and GL interrupted with Gaussian 09 software using B3LYP method 6-311++G(d, p) basis set³³⁻³⁵. The HOMO, LUMO and energy gap of 2PH molecules value is 6.266 eV, the IA compound value is 9.058 eV and the third compound GL energy value is 8.544 eV and presented in (Fig. 4), which three compounds comparatively the IA and GL energy gap have (9.058 and 8.544 eV) maximum values, thereby both compound have high stability molecules and low reactivity consider to be soft molecules. Similarly, the small energy gap of the 2PH compound has large reactivity and less stability considered hard

Table 2 — Molecular property of 2PH, IA, and GL components by B3LYP/6-311++G(d, p)

Parameters	2-Propanone, 1-hydroxy-	Isopropyl alcohol	Glycerin
Bond Angle Low (°)	(C ₂ -C ₁ -H ₇) → 107.08	(C ₂ -C ₁ -O ₄) → 106.24	(C ₃ -O ₄ -H ₁₁) → 105.11
Bond Angle High (°)	(C ₁ -C ₂ -O ₄) → 122.60	(C ₂ -C ₁ -C ₃) → 112.52	(O ₁ -C ₂ -H ₈) → 111.86
Bond Length Low (Å)	(O ₅ -H ₁₁) → 0.96	(O ₄ -H ₁₂) → 0.96	(O ₆ -H ₁₄) → 0.96
Bond Length High (Å)	(C ₁ -C ₂) → 1.52	(C ₁ -C ₂) → 1.52	(C ₃ -C ₅) → 1.52
Mulliken Charge Negative (a.u)	O ₁ → -0.506	O ₄ → -0.526	O ₁ → -0.526
Mulliken Charge Positive (a.u)	H ₁₁ → 0.306	H ₁₂ → 0.298	H ₁₄ → 0.304
NBO Analysis Kcal/mol	LP(2) O ₄ → σ* C ₁ -C ₂ (22.99)	LP(2) O ₄ → σ* C ₁ -H ₅ (6.61)	LP(2) O ₄ → σ* C ₃ -C ₅ (6.51)
E _{HOMO} (eV)	-6.608	-7.097	-6.889
E _{LUMO} (eV)	-0.341	1.960	1.655
Ionization Potential (eV)	6.608	7.097	6.889
Electron Affinity (eV)	0.341	-1.960	-1.655
E _{HOMO} - E _{LUMO} (eV)	6.266	9.058	8.544
Fermi Energy or Electronegativity (eV)	3.474	2.568	2.616
Chemical Potential (eV)	-3.474	-2.568	-2.616
Chemical Hardness (eV)	3.133	4.529	4.272
Chemical Softness (eV ⁻¹)	0.319	0.220	0.234
Electrophilicity Index (eV)	1.926	0.728	0.801
Nucleophilicity Index (eV ⁻¹)	0.519	1.373	1.247
ΔNmax(eV)	1.094	0.560	0.612
Electron donating capability (eV)	4.056	2.578	2.643
Electron-accepting capability (eV)	0.581	0.010	0.027

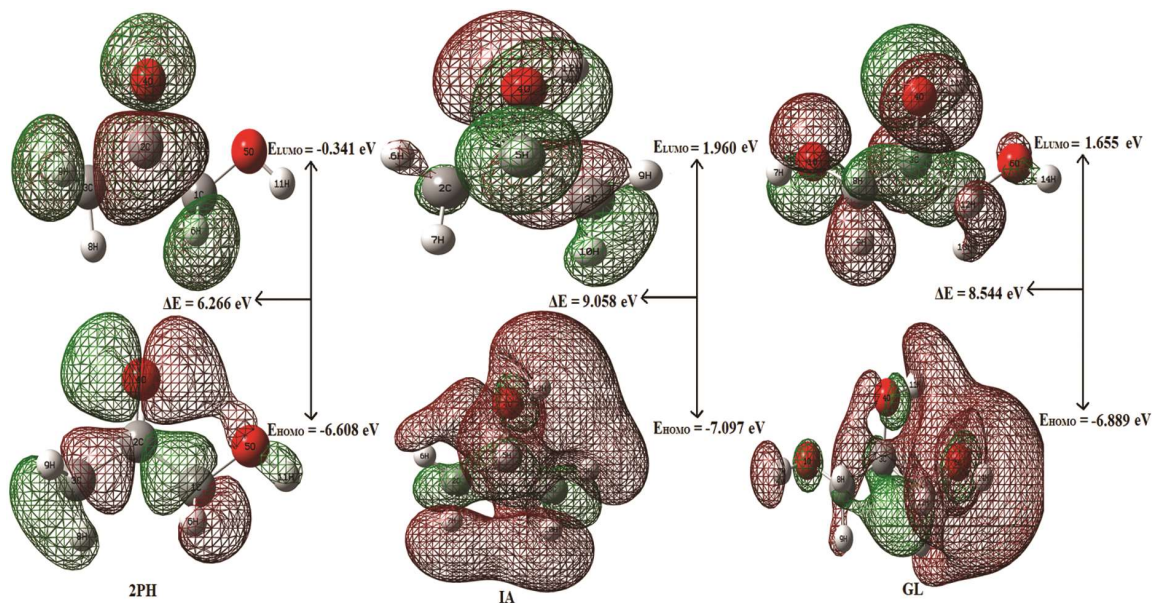


Fig. 4 — HOMO-LUMO plot on 2PH, IA and GL by B3LYP/6-311++G(d, p) basis set

molecules. The large and small energy gaps expressed relate to well biological activity, respectively. The ionization energy demonstrates an atom's capacity to lose the electrons (HOMO) whereas electron affinity energy describes the ability of an atom to gain the electrons (LUMO) from the title molecules^{36,37}. The chemical potential for 2PH, IA and GL compounds

was found to be -3.473, -2.553 and -2.617 eV, with a decrease in chemical potential value, leading to an increase in the reactive activity. A good electrophile is characterized by a greater value of the global electrophilicity index, while a good nucleophile is suggested by a lower value. According to the global classification analysis, 2PH molecules have global

electrophilicity measurements greater than 1.5 eV, which makes it an excellent electrophile. The greater global electrophilicity index value represents an excellent electrophile, while the lower number indicates an effective nucleophile³⁸. Outstanding biological function is demonstrated by the compound of 2PH has a lower nucleophilicity index (0.519 eV) as well as a higher electrophilicity index (1.926 eV) among the three components.

Natural bond analysis (NBO) analysis

The NBO technique is used to determine the electron recipients and donor engaged in the interaction, as well as how these relationships affect the long-term stability of the molecular strengths are calculated for three compounds (2PH, IA and GL) were performed functional level of method DFT/B3LYP/6-311++G(d, p) basic set³⁹. The number of the major donor-acceptor interactions along the corresponding E(2) stabilization energy, which considers the higher ionization energies of the C=O molecules is responsible for strong stabilization energy expressed in the three derivatives. This high ionization energy gives large stabilization to the 2PH, IA and GL compounds⁴⁰. Between donors (occupied) O₄ from acceptor (empty) C₁-C₂ which is increased highest intermolecular stabilization energy E(2) value found 22.99 Kcal mol⁻¹ on 2-propanone, 1-hydroxy-(2PH) molecules. Between donors (occupied) O₄ from acceptor (empty) C₁-H₅ which is increased highest intermolecular stabilization energy E(2) value found 6.61 Kcal mol⁻¹ on isopropyl alcohol (IA) molecules. Between donors (occupied) O₄ from acceptor (empty) C₃-C₅ which is increased highest intermolecular stabilization energy E(2) value found 6.51 Kcal mol⁻¹ on glycerin (GL) molecules. The larger stabilization energy E(2) value is three compounds due to lone pair LP(2) → σ* anti-bonding of 2PH compound, the next lone pair LP(2) → σ* anti-bonding of IA molecules and the last compound of GL molecules hyper conjugative interaction based on lone pair LP(2) → σ* anti-bonding, respectively.

Topological analysis

ELF, LOL and ESP investigation on three compounds

The topological parameters of ELF, LOL plots have been obtained by three organic optimized geometry compounds 2PH, IA and GL. The electron localized function (ELF), localized orbital locator (LOL) have similar predictions in chemical characteristics (non-covalent, bonding, non-bonding,

localization and delocalization) based on kinetic electron density⁴¹. Mostly, the LOL, ELF is used to estimate the biological reactivity among the atom and molecules. The plot ranges exhibit from 0.0 to 0.1 and 0.0 to 0.8, which consider bonding, and non-bonding of localized and delocalized (< 0.5) transfer on the electrons obtained by Multiwfn 3.7^{42,43} based on the same basic set as illustrated in (Fig. 5). The high LOL, ELF present around the hydrogen atoms, which associated as red color and maximum localization of electron whereas the low LOL, ELF has occupied nearby carbon atoms, that indicates as blue color and high delocalization electron cloud. The electron depletion zone located between the inner and valence layers is demonstrated by a blue circle surrounding the oxygen atoms on 2PH, IA and GL components. The total electrostatic potential (ESP) exhibits local minimum and maximum electron density, which plot region from -0.1 to +0.1 on title molecules⁴⁴. Therefore, the intra and inter-molecular charge of delocalization inside the molecules is illustrated by LOL, ELF maps that conformed through NBO, MEP and FMO analysis.

Non covalent interaction-reduced density gradient (NCI-RDG) analysis

The RDG technique has been employed in conjunction with the quantum theory on molecules to demonstrate the inter-intra molecular and covalent interactions according to the electron density developed by Johnson *et al.*⁴⁵. The process can identify repulsive steric interaction, hydrogen bonding and Van der Waals using basic color codes obtained multiwfn 3.8 program and structure illustrated using VMD 1.9.4 on 2PH, IA and GL components as depicted in (Fig. 6). The RDG iso-surface and NCI scatter plot shows ranges from -0.035 to +0.020 a.u., which observed the rich repulsion is represented by red zones ($\lambda_2 > 0$), high attraction is indicated by blue region ($\lambda_2 < 0$) and strong intermediate interaction denoted by green zones ($\lambda_2 \approx 0$) of title molecules^{46,47}. The strong localization and delocalization ranges predict 0.02 to 0.05 a.u and -0.02 to -0.05 a.u which correspond to bonding and non-bonding interaction occupied nearby hydrogen, and oxygen atoms on title molecules, which conformed well biological reactivity in the molecular system.

Thermodynamic properties on 2PH, IA and GL

The thermodynamic parameters of vibrational zero-point energy, entropy (S), capacity (V) and specific heat (H) are estimated by PERL-SCRIPT (thermo.pl)

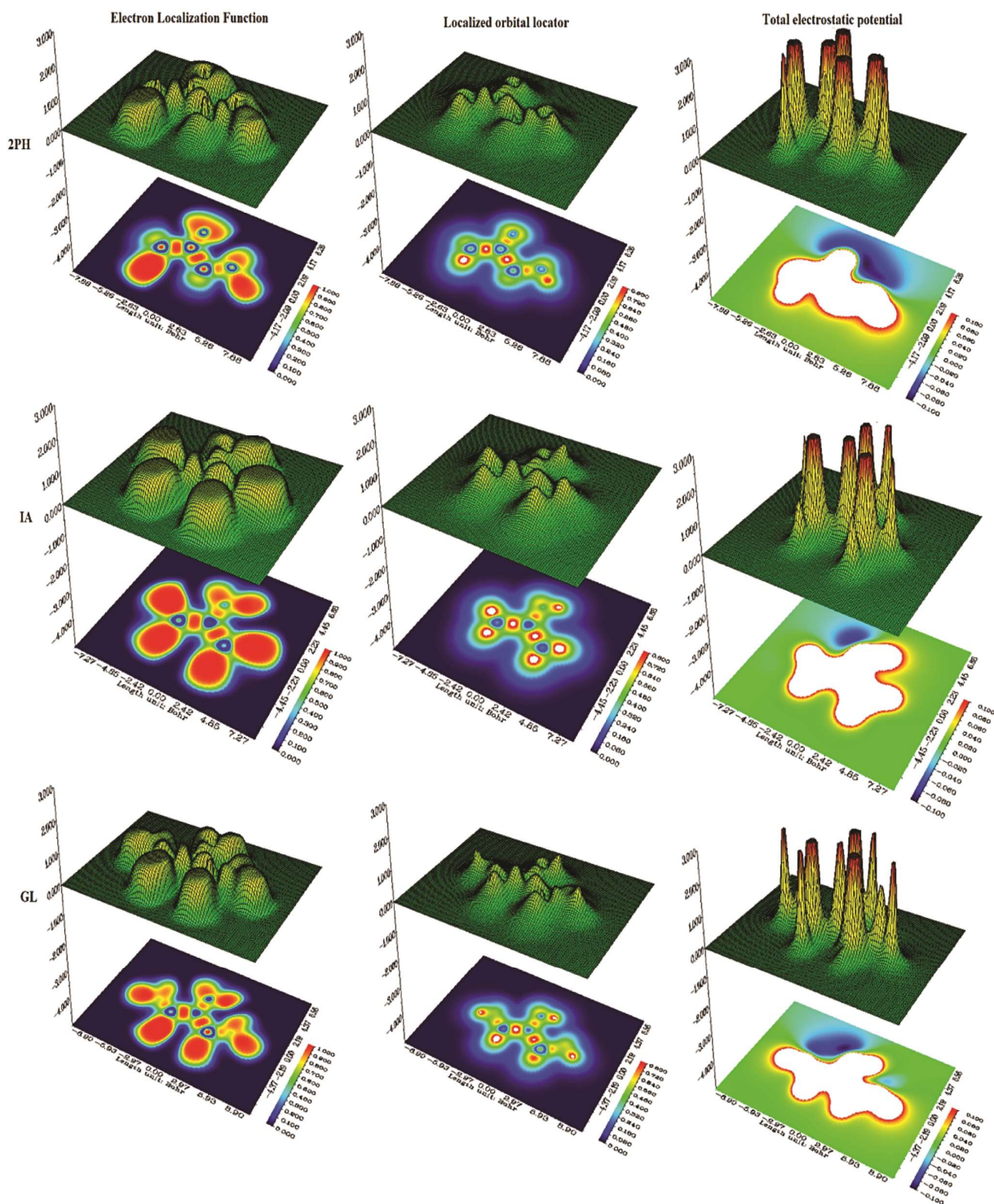
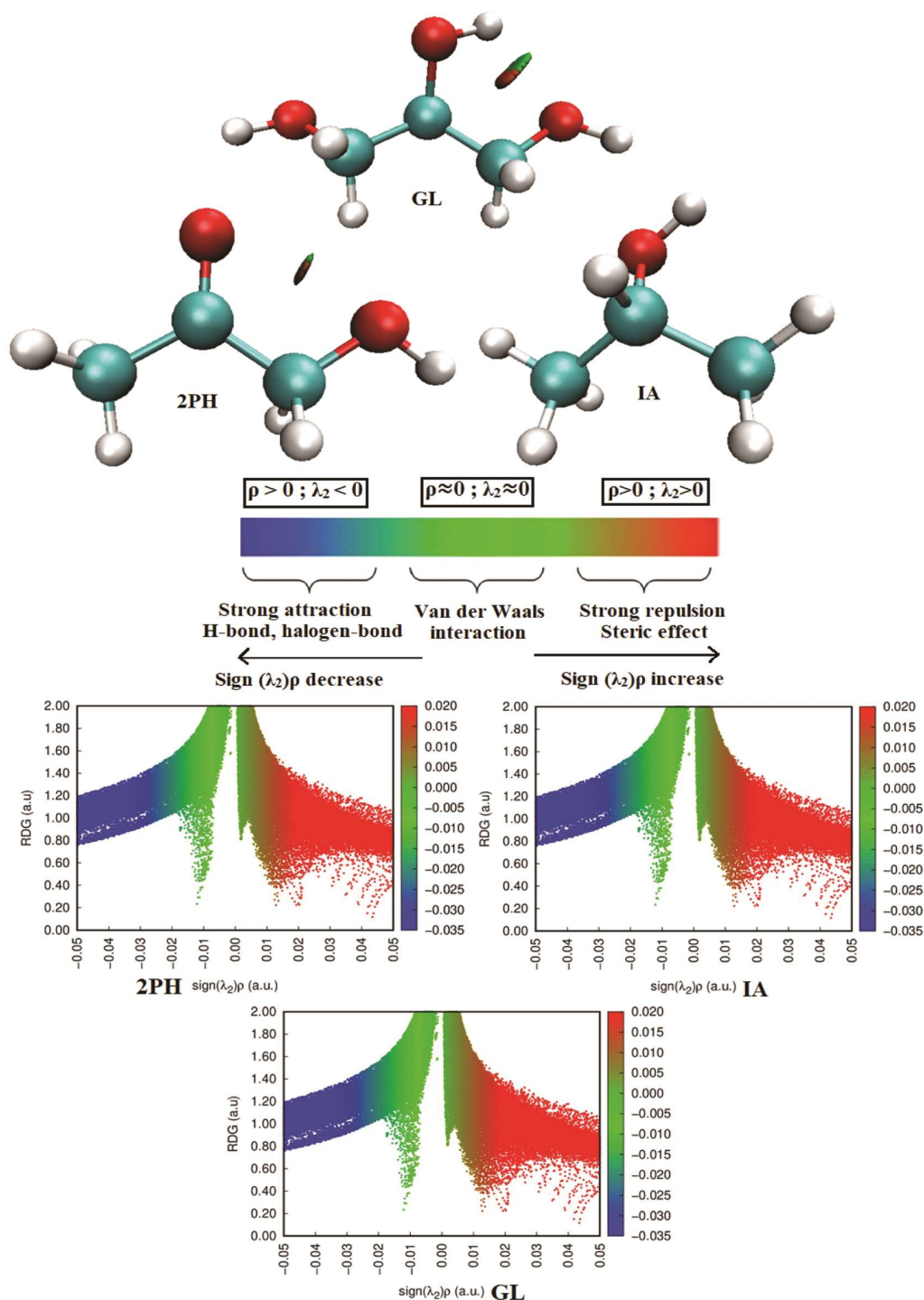


Fig. 5 — ELF, LOL schematic illustration of 2PH, IA and GL

based on hybrid accuracy B3LYP/6-311++G(d, p) set for optimized geometry structure at ground state⁴⁸, across the temperature lies between 100 K to 1000 K of 2PH, IA and GL molecules as depicted in (Table 3). The variation of temperature increases similar to vibrational energy

increases among the particles⁴⁹. The thermal energy applied in the function of S, C, and H also increased due to affected by the ground state vibrational motion of the molecules while increasing the temperature as illustrated in (Fig. 7). These characteristics are very essential to

Fig. 6 — Plot of RDG versus $\text{sign} \lambda_2$ for 2PH, IA and GL

studying increasing absorption in the drug design on optimized molecular and the receptor-binding interaction of the title compounds.

Nonlinear optical (NLO) Properties of 2PH, IA and GL

NLO plays a significant role in many fields, such as optical computer, optical signal processing,

telecommunication and precision metrology and laser surgery. In the present investigation, the NLO characteristics of 2PH, IA and GL compounds by evaluating their polarizability and dipole-moment have been obtained B3LYP/6-311++G(d, p) level are listed in (Table 4). In pharmaceuticals, drug

Table 3 — Thermodynamic properties on 2PH, IA and GL

T(K)	2-Propanone, 1-hydroxy-			Isopropyl alcohol			Glycerin		
	S (J/mol.K)	C (J/mol.K)	H (kJ/mol)	S (J/mol.K)	C (J/mol.K)	H (kJ/mol)	S (J/mol.K)	C (J/mol.K)	H (kJ/mol)
100	239.867	47.377	3.809	228.96	43.979	3.588	256.794	61.68	4.389
200	278.731	66.504	9.525	266.769	66.737	9.173	309.153	90.989	12.11
298.15	308.747	85.375	16.965	297.212	87.411	16.724	350.199	116.602	22.283
300	309.276	85.745	17.123	297.754	87.819	16.886	350.922	117.103	22.5
400	336.683	105.628	26.698	326.064	110.025	26.78	388.325	144.062	35.566
500	362.25	123.79	38.189	352.882	130.697	38.837	423.165	168.505	51.224
600	386.236	139.366	51.369	378.34	148.643	52.827	455.766	189.11	69.137
700	408.737	152.555	65.983	402.437	164.007	68.479	486.244	206.251	88.931
800	429.861	163.786	81.814	425.223	177.24	85.558	514.752	220.656	110.296
900	449.723	173.426	98.687	446.777	188.724	103.869	541.469	232.931	132.991
1000	468.436	181.75	116.456	467.191	198.738	123.253	566.572	243.506	156.826

Table 4 — Dipole moment (μ) Polarizability (α) of 2PH, IA and GL components

2-Propanone, 1-hydroxy-		Isopropyl Alcohol		Glycerin	
Parameters	B3LYP/6-311++G(d, p)	Parameters	B3LYP/6-311++G(d, p)	Parameters	B3LYP/6-311G++(d, p)
μ_x	-0.052	μ_x	1.135	μ_x	1.294
μ_y	-4.105	μ_y	-0.632	μ_y	-2.625
μ_z	0.004	μ_z	0.805	μ_z	1.680
μ_{tot}	5.620	μ_{tot}	0.779	μ_{tot}	3.797
α_{xx}	52.679	α_{xx}	39.895	α_{xx}	43.768
α_{xy}	0.574	α_{xy}	1.285	α_{xy}	-0.142
α_{yy}	41.603	α_{yy}	38.160	α_{yy}	40.913
α_{xz}	-0.132	α_{xz}	0.491	α_{xz}	0.003
α_{yz}	-0.717	α_{yz}	-0.248	α_{yz}	-0.002
α_{zz}	37.859	α_{zz}	34.163	α_{zz}	28.789
	44.047		37.406	α_{tot}	37.823

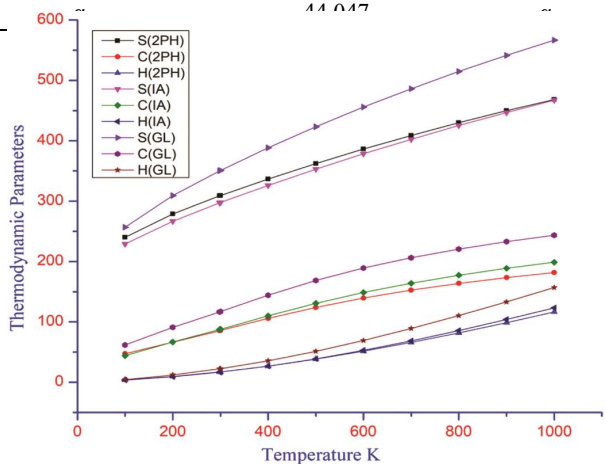


Fig. 7 — Thermodynamic Properties of 2PH, IA and GL

development and the industry are examined by using the polarizability (α)⁵⁰. The dipole moment is one of the crucial elements to predict the structural bio-chemistry, which useful classification for describing how the electrons travel throughout the molecules. When the molecules have charge transfer from the ground state to a higher state, the result of

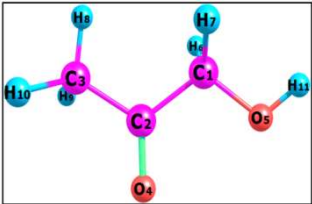
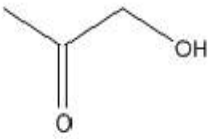
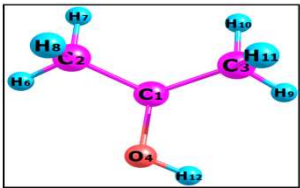
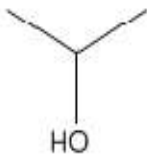
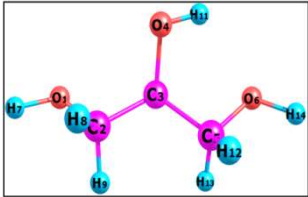
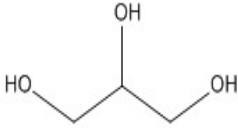
highest state molecules has a larger dipole-moment (μ) than ground state molecules⁵¹. The change of $\Delta\mu$ after excitation, which expresses the dynamics of emission state or intermolecular charge transfer (ICT). The following is the definition of the dipole moment (μ) and polarizability (α) estimated as:

$$\mu_{tot} = \sqrt{(\mu_x^2 + \mu_y^2 + \mu_z^2)}$$

$$\alpha_{tot} = \frac{\alpha_{xx} + \alpha_{yy} + \alpha_{zz}}{3}$$

The three components 2PH, IA and GL exhibit the largest dipole moment value in the way of direction μ_z , μ_x and μ_y , which is equivalent to 5.620D, 0.779D and 3.797D, among the three compounds, the 2-Propanone, 1-hydroxy- has high amount of dipole moment. Similarly, the polarizability of the three components has been estimated by 44.047×10^{-24} e.s.u (2PH), 37.406×10^{-24} e.s.u (IA) and 37.823×10^{-24} e.s.u (GL), among the three, the 2-propanone,

Table 5 — 2D and 3D structure of three compounds 2PH, IA, and GL

Compound name	3D structure	2D structure	Compounds formula
2-Propanone, 1-hydroxy-			$C_3H_6O_2$
Isopropyl alcohol			C_3H_8O
Glycerin			$C_3H_8O_3$

1-hydroxy- has contained high amount of polarizability, which indicates high efficient NLO material. The calculated polarizability and dipole moment of 2PH, IA and GL compounds greater than 10 times and 15 times of their urea 1.3738 Debye and 3.8312×10^{-24} esu⁵², that urea is frequently employed as a reference for describing organic nonlinear optical substances. According to these findings, the 2PH compound has strong nonlinear characteristics and would be an excellent choice for use in optical device designs.

Topological aspects of 2D structure of three compounds

The three chemical-optimized structures convert into the molecular graph (G) with edges and vertices in the theoretical chemistry. The number of edges incident to a vertex i is called the degree $d_G(i)$ and the distance degree $d_G(i, j)$ between any pair of vertices $\{i, j\}$ in G is the length of the shortest path connecting these two vertices. The goal of the present study we were to investigate QSAR/QSPR method in different degree-based topological descriptors on pharmacological activity theoretically⁵³⁻⁵⁶. The topological indicators calculated from the fundamental interaction of the 2D substances of optimized structure may demonstrate essential correlations to the physical characteristics of

these compounds by the quality of structure-activity, properties and harmful effects interactions. The topological indices⁵⁷ used to predict quantitative of three molecular structures namely 2-propanone, 1-hydroxy- contain the compound formula $C_3H_6O_2$ and compound weight 74.08 g/mol. Isopropyl alcohol consists of compound formula C_3H_8O and compound weight 60.1 g/mol and glycerin, which compound formula $C_3H_8O_3$ and compound weight 92.09 g/mol, two dimensional and three dimension structures as given in (Table 5). Using various degree-based topological indices defined as Randic χ (G), Zagreb M_1 (G) and M_2 (G), Atom bond connectivity ABC (G), Sum connectivity SC(G), Geometric arithmetic GA (G), Harmonic H (G), third Zagreb ZG_3 (G), Second Hyper-Zagreb HM_2 (G), Forgotten F(G), and Symmetric division deg SSD(G) in chemical graph theory which numerous values correlated with physical properties such as boiling point ($^{\circ}C$), melting point, molar refractivity (cm^3), polarity (cm^3), polar surfaces area (A^2) and complexity based on pharmacological activity in chemical descriptors. The above-mentioned 10 degree-based topological indices are suitable for studying drug discovery that is used to prevent enormous biological activity.

Definitions and literature review

Definition 1— The Randic index has been widely used by the topological index in chemical reactions and drug applications, especially in QSAR/QSPR research used in extremal trees with domination numbers⁵⁸. Developed by Randic denoted by graph G having vertex set $V(G)$ and edge set $E(G)$ given below:

$$\chi(G) = \sum_{ij \in E(G)} \frac{1}{\sqrt{d_i d_j}}$$

Definition 2— The Gutman and Trinajestic established the Zagreb indices almost thirty decades earlier⁵⁹. The first and second Zagreb indices as follows:

$$M_1(G) = \sum_{ij \in E(G)} (d_i + d_j)$$

and

$$M_2(G) = \sum_{ij \in E(G)} d_i d_j$$

Definition 3 — The ABC index was established by Estrada *et al.* in 1998 and has been applied to the investigation of the strength of alkanes and strain energy of cycloalkanes⁶⁰. The ABC index is defined as:

$$ABC(G) = \sum_{ij \in E(G)} \sqrt{\left(\frac{d_u + d_v - 2}{d_i d_j} \right)}$$

Definition 4—The growing popularity of the connection index has contributed to the inclusion of several variations in the literature survey. The two connection index sum-connectivity and atom-bond sum-connectivity index have been focused on in the biological prediction of extensive research. Developed the ABC index by utilizing the basic concept of the SC index⁶¹. The new variant of the SC index is defined as:

$$SC(G) = \sum_{ij \in E(G)} \frac{1}{\sqrt{d_i + d_j}}$$

Definition 5—The GA index of geometricarithmetic was discovered by Vukicevic and Furtula, which was inspired by the concept of the Randic connectivity index. Additionally, Vukicevic and Furtula provided the upper and lower limits of GA index and conformed the trees with the lowest

and highest GA indices through the star and the path respectively⁶². The new geometricarithmetic of (GA) is used to predict physical characteristic defined by:

$$GA(G) = \sum_{ij \in E(G)} \frac{2\sqrt{d_i d_j}}{d_i + d_j}$$

Definition 6 —The Harmonic index is also known as Randic index first invented by Favaron *et al.*⁶³. The new Harmonic index of $H(G)$ used to predict physical properties defined as:

$$H(G) = \sum_{ij \in E(G)} \frac{2}{d_i + d_j}$$

Definition 7—Since the third Zagreb indices were first described by Gutman *et al.*⁶⁴. Over forty years ago, another variation of these topological indices has been created as:

$$ZG_3(G) = \sum_{e=ij \in E(G)} |d_i - d_j|$$

Definition 8—The topological index of the second Hyper-Zagreb index is the one that describes the actual molecular features. The HM_2 index contains several graphs and bounds are estimated. Additionally, linear regression investigation of degree-based with physical characteristics of a boiling point of benzenoid hydrocarbons was interpreted by literature review^{65,66}. The second Hyper-Zagreb index of graph $HM_2(G)$ is as follows:

$$HM_2(G) = \sum_{ij \in E(G)} (d_i + d_j)^2$$

Definition 9—The Forgotten topological index and the first Zagreb index are nearly identical proposed by Furtula and Gutman⁶⁷. The F-index plays a very important role in predicting the chemical stability and medicinal properties of new drug molecular structures. The F-topological index of graph $F(G)$ is stated as:

$$F(G) = \sum_{ij \in E(G)} [(d_i)^2 + (d_j)^2]$$

Definition 10 —A few decades back Vukicevic and Gasperov examined a novel class biological descriptor of symmetric division deg (SDD) topological index⁶⁸. The symmetric division deg graph SSD (G) is stated as:

Table 6 — Physical property on 2PH, IA, and GL components

Name of the compound	Boiling point (°C)	Melting point (°C)	Flash point (°C)	Polar surface area(A ²)	Complexity	Molar refractivity (cm ³)	Polarity (cm ³)
2-propanone, 1-hydroxy-	145	-17	56	37.3	59.8	17.9	7.26
Isopropyl alcohol	82.3	-89.5	12	20.23	10.8	17.4	7.14
Glycerin	290	20	177	60.7	25.2	17.5	7.19

$$SDD = SSD(G) = \sum_{ij \in E(G)} \left[\frac{d_i^2 + d_j^2}{d_i d_j} \right]$$

The main objective of this investigation, we describe ten degree-based topological indices used to predict the physical quality of three molecular graphs and correlated physical-chemical properties of boiling point (°C), melting point, flash point (°C), molar refractivity (cm³), polarity (cm³), polar surfaces are (A²) and complexity⁶⁹ of three natural chemical structure identified from GC-MS recorded. The seven physical properties values have been taken from PubChem website under the national library of medicine as shown in (Table 6), respectively.

Mathematical aspects of three (2PH, IA and GL) compounds

In this section, utilizing the definition of topological index provides the proof and the essential result stated as follows mainly based on graph chemical structure.

Theorem 1.1 — The ten degree-based topological indices of the molecular graph 2-propanone, 1-hydroxy (2PH) are $\chi(2PH) = 2.268$, $M_1(2PH) = 16$, $M_2(2PH) = 14$, $ABC(2PH) = 3.038$, $SC(2PH) = 2.024$, $GA(2PH) = 4.791$, $H(2PH) = 2.066$, $ZG_3(2PH) = 06$, $HM_2(2PH) = 66$, $F(2PH) = 38$, and $SSD(2PH) = 11.332$.

Proof: Let G be the graph of 2PH and $E(i, j)$ denote the class of edges of G connecting vertices with degree i to degree j . From the neglected hydrogen of 2PH chemical structure observe the number of edges and vertices that $|E_{1,3}| = 2$, $|E_{3,2}| = 1$ and $|E_{2,1}| = 1$.

(i) The result of using principle 1 is as follows:

$$\chi(2PH) = 2 \frac{1}{\sqrt{1.3}} + \frac{1}{\sqrt{3.2}} + \frac{1}{\sqrt{2.1}} = 2.268.$$

(ii) The result of using definition 2 is as follows:

$$M_1(2PH) = 2(1+3) + (3+2) + (2+1) = 16.$$

and

$$M_2(2PH) = 2(3) + 6 + 2 = 14.$$

(iii) The result of using definition 3 is as follows:

$$ABC(2PH) = 2 \sqrt{\left(\frac{1+3-2}{1.3}\right)} + \sqrt{\left(\frac{3+2-2}{3.2}\right)} + \sqrt{\left(\frac{2+1-2}{2.1}\right)} = 3.038.$$

(iv) By using the theorem 4, the following results are obtained:

$$SC(2PH) = 2 \frac{1}{\sqrt{1+3}} + \frac{1}{\sqrt{3+2}} + \frac{1}{\sqrt{2+1}} = 2.024.$$

(v) By using the definition 5, that following results are obtained:

$$GA(2PH) = 2 \left(\frac{2\sqrt{1.3}}{1+3} \right) + \left(\frac{2\sqrt{3.2}}{3+2} \right) + \left(\frac{2\sqrt{2.1}}{2+1} \right) = 4.791.$$

(vi) By using principle 6, we get the result obtained:

$$H(2PH) = 2 \left(\frac{2}{1+3} \right) + \left(\frac{2}{3+2} \right) + \left(\frac{2}{2+1} \right) = 2.066.$$

(vii) By using definition 7, we get the following:

$$ZG_3(2PH) = 2|1-3| + |3-2| + |2-1| = 06$$

(viii) By using theorem 8, we get the following:

$$HM_2(2PH) = 2(1+3)^2 + (3+2)^2 + (2+1)^2 = 66.$$

(ix) By using principle 9, we get the following:

$$F(2PH) = 2[1^2 + 3^2] + [3^2 + 2^2] + [2^2 + 1^2] = 38.$$

(x) By using definition 10, we get the following:

$$SSD(2PH) = 2 \left[\frac{1}{3} + \frac{3}{1} \right] + \left[\frac{2}{3} + \frac{3}{2} \right] + \left[\frac{1}{2} + \frac{2}{1} \right] = 11.332.$$

Theorem 1.2 — The ten degree-based topological indices of G are listed below if G is the molecular graph of isopropyl alcohol (IA) given as $\chi(IA) = 1.731$, $M_1(IA) = 12$, $M_2(IA) = 09$, $ABC(IA) = 2.448$, $SC(IA) = 1.5$, $GA(IA) = 2.598$, $H(IA) = 1.5$, $ZG_3(IA) = 06$, $HM_2(IA) = 48$, $F(IA) = 30$, and $SSD(IA) = 9.999$.

Proof: Let G be the graph of IA and $E(i, j)$ denote the class of edges of G connecting vertices with degree i to degree j . From the neglected hydrogen of IA chemical structure observe the number of edges and vertices that $|E_{1,3}| = 3$.

(i) The result of using principle 1 is as follows:

$$\chi(IA) = 3 \frac{1}{\sqrt{1.3}} = 1.731.$$

(ii) The result of using definition 2 is as follows:

$$M_1(IA) = 3(1+3) = 12.$$

and

$$M_2(IA) = 3(3) = 09.$$

(iii) The result of using definition 3 is as follows:

$$ABC(IA) = 3 \sqrt{\left(\frac{1+3-2}{1.3}\right)} = 2.448.$$

(iv) By using the theorem 4, the following results are obtained:

$$SC(IA) = 3 \frac{1}{\sqrt{1+3}} = 1.5.$$

(v) By using principle 5, the following results are obtained:

Table 7 — Estimated topological index (G = 2PH, IA and GL)

Topological indices	2-Propanone, 1-hydroxy-	Isopropyl alcohol	Glycerin
Randic index $\chi(G)$	2.268	1.731	2.805
Zagreb index $M_1(G)$	16	12	09
Zagreb index $M_2(G)$	14	09	19
Atom bond connectivity ABC(G)	3.038	2.448	3.644
Sum connectivity SC(G)	2.024	1.5	2.548
Geometric arithmetic GA(G)	4.791	2.598	19
Harmonic H(G)	2.066	1.5	2.632
third Zagreb $ZG_3(G)$	06	06	06
Second Hyper-Zagreb $HM_2(G)$	66	48	84
Forgotten F(G)	38	30	46
Symmetric division deg SSD(G)	11.332	9.999	12.665

$$GA(IA) = 3\left(\frac{2\sqrt{1.3}}{1+3}\right) = 2.598.$$

(vi) By using principle 6, we get the result obtained:

$$H(IA) = 3\left(\frac{2}{1+3}\right) = 1.5.$$

(vii) By using definition 7, we get the following:

$$ZG_3(IA) = 3|1 - 3| = 06$$

(viii) By using theorem 8, we get the following:

$$HM_2(IA) = 3(1 + 3)^2 = 48.$$

(ix) By using principle 9, we get the following:

$$F(IA) = 3[1^2 + 3^2] = 30.$$

(x) By using definition 10, we get the following:

$$SSD(IA) = 3\left[\frac{1}{3} + \frac{3}{1}\right] = 9.999.$$

Theorem 1.3 — The ten degree-based topological indices of the molecular graph glycerin (GL) are $\chi(GL) = 2.805$, $M_1(GL) = 20$, $M_2(GL) = 19$, $ABC(GL) = 3.644$, $SC(GL) = 2.548$, $GA(GL) = 4.709$, $H(GL) = 2.632$, $ZG_3(GL) = 06$, $HM_2(GL) = 84$, $F(GL) = 46$, and $SSD(GL) = 12.665$.

Proof: Let G be the graph of GL and $E(i, j)$ denote the class of edges of G connecting vertices with degree i to degree j. From the neglected hydrogen of GL chemical structure observe the number of edges and vertices that $|E_{1,2}| = 2$, $|E_{3,2}| = 2$ and $|E_{3,1}| = 1$.

(i) The result of using principle 1 is as follows:

$$\chi(GL) = 2\frac{1}{\sqrt{1.2}} + 2\frac{1}{\sqrt{3.2}} + \frac{1}{\sqrt{3.1}} = 2.805.$$

(ii) The result of using definition 2 is as follows:

$$M_1(GL) = 2(1+2) + 2(3+2) + (3+1) = 20.$$

and

$$M_2(GL) = 2(2) + 2(6) + 3 = 19.$$

(iii) The result of using definition 3 is as follows:

$$ABC(GL) = 2\sqrt{\left(\frac{1+2-2}{1.2}\right)} + 2\sqrt{\left(\frac{3+2-2}{3.2}\right)} + \sqrt{\left(\frac{3+1-2}{3.1}\right)} = 3.644.$$

(iv) By using the theorem 4, the following results are obtained:

$$SC(GL) = 2\frac{1}{\sqrt{1+2}} + 2\frac{1}{\sqrt{3+2}} + \frac{1}{\sqrt{3+1}} = 2.548.$$

(v) By using principle 5, the following results are obtained:

$$GA(GL) = 2\left(\frac{2\sqrt{1.2}}{1+2}\right) + \left(\frac{2\sqrt{3.2}}{3+2}\right) + \left(\frac{2\sqrt{3.1}}{3+1}\right) = 4.709.$$

(vi) By using principle 6, we get the result obtained:

$$H(GL) = 2\left(\frac{2}{1+2}\right) + 2\left(\frac{2}{3+2}\right) + \left(\frac{2}{3+1}\right) = 2.632.$$

(vii) By using definition 7, we get the following:

$$ZG_3(GL) = 2|1 - 2| + 2|3 - 2| + |3 - 1| = 06$$

(viii) By using theorem 8, we get the following:

$$HM_2(GL) = 2(1 + 2)^2 + 2(3 + 2)^2 + (3 + 1)^2 = 84.$$

(ix) By using principle 9, we get the following:

$$F(GL) = 2[1^2 + 2^2] + 2[3^2 + 2^2] + [3^2 + 1^2] = 46.$$

(x) By using definition 10, we get the following:

$$SSD(GL) = 2\left[\frac{1}{2} + \frac{2}{1}\right] + 2\left[\frac{2}{3} + \frac{3}{2}\right] + \left[\frac{1}{3} + \frac{3}{1}\right] = 12.665.$$

Finally, the result of associated values of the physical characteristics of three bio-activity compounds with established degree-based ten topological indices (Tables 6 & 7). The following result, when contracted to other indices, is possibly viewed that $M_1(G) = 20$ index exhibits a most significant positive association with melting point $^{\circ}C = 20$ and $ZG_3(G) = 06$ index shows a favourable correlation with physical properties of polarity $cm^3 = 7.19$ in the graph G glycerine chemical structure. Similarly, $ZG_3(G) = 06$ and $SSD(G) = 9.99$ indices values have the strongest positive agreement with polarity and complexity in graph G of isopropyl alcohol. The polarity of chemical graph G of 2-propanone, 1-hydroxy- highly well matched with third Zagreb topological indices. Therefore, it can be noted that estimated degree-based topological indices are

extremely associated with experimental physical characteristic values of natural bio-activity compounds. The above mathematical results of the three compounds proved through topological indices correlated with experimental values that can be used without lab and reduce market price in the drug design of the medicinal field, respectively. The computation of other molecular in variants of 2PH, IA and GL might make for a fascinating study subject in the coming years.

Conclusion

In this work, we report GC-MS results on 2PH, IA and GL compounds were investigated the structural conformation, molecular behavior, stability, chemical reactivity, and electronic and optical properties obtained by B3LYP/6-311++G(d, p) level. The geometry-optimized structure expressed the highest and lowest bond angle, and bond length predicted by chemical properties. The Mulliken charge exhibits positive charge occupied around hydrogen atom $H_{11} \rightarrow 0.306(2PH)$, $H_{12} \rightarrow 0.298(IA)$ and $H_{14} \rightarrow 0.304(GL)$ a.u, and negative charge hold nearby oxygen atom $O_1 \rightarrow -0.506(2PH)$, $O_4 \rightarrow -0.526(IA)$ and $O_1 \rightarrow -0.526(GL)$ a.u of the molecules, which describes charge distribution and electron density. The HOMO-LUMO kinetic energy of $IA \rightarrow 9.058$, $GL \rightarrow 8.544$ eV, which demonstrated high stability, low reactivity as soft molecules and $2PH \rightarrow 6.266$ eV, which was associated with less stability, large reactivity as hard molecules with global descriptors also discussed, which expressed well biological properties. NBO examined the highest intermolecular stabilization energy $E(2)$ values $2PH=22.99$, $IA=6.61$ and $GL=6.51$ Kcal mol⁻¹. The LOL, ELE have demonstrated low and high localization and delocalization of the molecules. The RDG isosurface and non-covalent interaction (NCI) scatter plot showed repulsion ($\lambda_2 > 0$), attraction ($\lambda_2 < 0$) and strong intermediate interaction ($\lambda_2 \approx 0$), which conformed well to biological reactivity. Thermodynamic parameters and dipole moment = 5.620 Debye, polarizability = 44.047×10^{-24} e.s.u also computed, which associated excellent NLO properties. Furthermore, the estimated degree-based ten topological indices are extremely associated with experimental physical characteristic values of natural bio-activity compounds, which reduce market price for drug design in the medicinal field.

Conflict of interest

All authors declare no conflict of interest.

References

- 1 Yaylayan VA, Harty MS & Ismail AA, Monitoring Carbonyl–Amine Reaction and Enolization of 1-Hydroxy-2-propanone (Acetol) by FTIR Spectroscopy. *J Agric Food Chem*, 47 (1999) 2335.
- 2 Varoujan AY, Susan HM, & Ashraf AI, Monitoring Carbonyl-Amine Reaction and Enolization of 1-Hydroxy-2-propanone (Acetol) by FTIR Spectroscopy. *J Agric Food Chem*, 47 (1999) 2335.
- 3 Thomas Hofmann & Peter Schieberle, 2-Oxopropanal, Hydroxy-2-propanone, and 1-Pyrrolines Important Intermediates in the Generation of the Roast-Smelling Food Flavor Compounds 2-Acetyl-1-pyrroline and 2-Acetyltetrahydropyridine. *J Agric Food Chem*, 46 (1998) 2270.
- 4 Jammalamadaka D & Raissi S, Ethylene Glycol, Methanol and Isopropyl Alcohol Intoxication. *Am J Med Sci*, 339 (2010) 276.
- 5 Zhaoyou Z, Ying X, Huiyuan L, Yuanyuan S, Dapeng M, Peizhe C, Yixin M, Yinglong W & Jun G, Separation of isopropyl alcohol and isopropyl ether with ionic liquids as extractant based on quantum chemical calculation and liquid-liquid equilibrium experiment. *Sep Purif Technol*, 247 (2020) 116937.
- 6 Lillian CB, Wilma FB, Donald VB, Ronald AH, Curtis DK, Daniel CL, James GMJ, Ronald CS, Thomas JS, Paul WS, Lillian JG & Bart H, Safety Assessment of Glycerin as Used in Cosmetics. *Int J Toxicol*, 38 (2019) 820.
- 7 Muhammad WR, Abid M, Iqra H, An Estimation of the Physicochemical Properties of Heart Attack Treatment Medicines by Using Molecular Descriptors. *S Afr J Chem Eng*, 45 (2023) 20.
- 8 Rifat HM, Ahad AA, Burhan ZF, Mohammad HRM, Amer HA, Afsar ASM, Moon NP, Foysal A & Bonglee K, Application of Mathematical Modeling and Computational Tools in the Modern Drug Design and Development Process. *Molecules*, 27 (2022) 169.
- 9 Sangeetha N, Vaishnavi J, Manisha P, Ramkumar K & Sabina EP, Antioxidant mediated defensive potency of *Caesalpinia bonducella* nut on Acetaminophen-inbred spleen and cardiotoxicity: Implications on oxidative stress and tissue morphology in an *in vivo* model. *Indian J Biochem Biophys*, 60 (2023) 297.
- 10 Biplob KB, Mirza MAB, Amit S, Eliva J & Srinivas HG, Anti-proliferating effect of *Ocimum sanctum* and *Centella asiatica* plant extract on growth of human glioblastoma cells: An *in vitro* study. *Indian J Biochem Biophys*, 59 (2022) 956.
- 11 Sayyeda F, Yamuna K, Ramya G, Lahari PM, Priyanka LD & Dhanabal SP, Phytochemical evaluation and anti-proliferative activity of the ethanolic extract of the leaves of *Thespesia populnea*. *Indian J Biochem Biophys*, 59 (2022) 156.
- 12 Jain PK, Anjali S, Preeti J & Jeetendra B, Phytochemical analysis of *Mentha spicata* plant extract using UV-VIS, FTIR and GC/MS technique. *J Chem Pharm Res*, 8 (2016) 1.
- 13 Ukwubilea CA, Ahmeda A, Katsayal UA, Yaub J & Mejidac S, GC–MS analysis of bioactive compounds from *Melastomastrum capitatum* (Vahl) Fern. Leaf methanol extract: An anticancer plant. *Sci Afr*, 3 (2019) e00059.
- 14 Gregory S, Sandeepkumar K, Jens M & Edward WL, Computational Methods in Drug Discovery. *Pharmacol Rev*, 66 (2014) 334.

- 15 Philip BC & Rishi G, Contemporary Computational Applications and Tools in Drug Discovery. *ACS Med Chem Lett*, 13 (2022) 1016
- 16 Parvez A, Syed AKK, Osamah AR & Faizul A, Degree-based topological indices and polynomials of hyaluronic acid-curcumin conjugates. *Saudi Pharm J*, 28 (2020) 1093.
- 17 Adnan A, Yasir B, Safyan A & Wei G, On topological indices of certain dendrimer structures. *Z. Naturforsch*, 72 (2017) 559.
- 18 Frisch MJ, Trucks GW, Schlegel HB, Scuseria GE, Robb MA, Cheeseman JR, Scalmani G, Barone V, Mennucci B, Petersson GA, Nakatsuji H, Caricato M, Li, X, Hratchian HP, Izmaylov AF, Bloino J, Zheng G, Sonnenberg JL, Hada M, Ehara M, Toyota K, Fukuda R, Hasegawa J, Ishida M, Nakajima T, Honda Y, Kitao O, Nakai H, Vreven T, Montgomery JA, Peralta JE, Ogliaro F, Bearpark M, Heyd JJ, Brothers E, Kudin KN, Staroverov VN, Kobayashi R, Normand J, Raghavachari K, Rendell A, Burant JC, Iyengar SS, Tomasi J, Cossi M, Rega N, Millam JM, Klene M, Knox JE, Cross JB, Bakken V, Adamo C, Jaramillo J, Gomperts R, Stratmann RE, Yazyev O, Austin AJ, Cammi R, Pomelli C, Ochterski JW, Martin RL, Morokuma K, Zakrzewski VG, Voth GA, Salvador P, Dannenberg JJ, Dapprich S, Daniels AD, Farkas O, Foresman JB, Ortiz JV, Cioslowski J & Fox DJ, Gaussian 09, Revision B.01. *Gaussian Inc*, Wallingford (2010).
- 19 Mehmet K, Etem K, Ahmet A, Abdullah MA & Mustafa K, Monomeric and dimeric structures analysis and spectroscopic characterization of 3, 5-difluorophenylboronic acid with experimental (FT-IR, FT-Raman, ¹H and ¹³C NMR, UV) techniques and quantum chemical calculations. *J Mol Struct*, 1058 (2014) 79.
- 20 Siyamak S, Masoome S, Mehrnoosh K, Iryna B & Fatemeh A, DFT Study of Physisorption Effect of the Curcumin on CNT(8, 0-6) Nanotube for Biological Applications. *Chinese J Struct Chem*, 38 (2019) 37.
- 21 Jai KO, Gaddam R & Byru VR, Structure, chemical reactivity, NBO, MEP analysis and thermodynamic parameters of pentamethyl benzene using DFT study. *Chem Phys Impact*, 7 (2023) 100280.
- 22 Kanchana S, Kaviya T, Rajkumar P, Dhinesh KM, Elangovan N & Sowrirajan S, Computational investigation of solvent interaction (TD-DFT, MEP, HOMO-LUMO), wavefunction studies and molecular docking studies of 3-(1-(3-(5-((1-methylpiperidin-4-yl) methoxy) pyrimidin-2-yl) benzyl) -6-oxo-1, 6-dihydropyridazin-yl) benzonitrile. *Chem Phys Impact*, 7 (2023) 100263.
- 23 Kanagaraj J, Sivarajani V, Pavithra U, Sridhar J & Lakshmanan M, Computational studies on new Leishmanial drug targets against Quercetin. *Indian J Biochem Biophys*, 59 (2022) 909.
- 24 Habib RM, Muthu S, Raajaraman BR, Raja M, H. Umamaheswari, Investigations on 2-(4-Cyanophenylamino) acetic acid by FT-IR, FT-Raman, NMR and UV-Vis spectroscopy, DFT (NBO, HOMO-LUMO, MEP and Fukui function) and molecular docking studies, *Heliyon*, 6 (2020) e04976.
- 25 Ranjan KM, Kuldeep D, Amr Ahmed EA, Ashish KS, Ruchi T, Talha BE, Mohammad A, Saud IAR, Mukesh KR, Veronique S & Mohnad A, Repurposing benzimidazole and benzothiazole derivatives as potential inhibitors of SARS-CoV-2: DFT, QSAR, molecular docking, molecular dynamics simulation, and in-silico pharmacokinetic and toxicity studies. *J King Saud Univ Sci*, 33 (2021) 101637.
- 26 Eswaraiiah G, Abraham PK, Krupanidhi S, Bharath KR & Venkateswarulu TC, Identification of bioactive compounds in leaf extract of *Avicennia alba* by GC-MS analysis and evaluation of its in-vitro anticancer potential against MCF7 and HeLa cell lines. *J King Saud Univ Sci*, 32 (2020) 740.
- 27 Ahmed AJ, Fuad OA, Kamaran KA, Yaseen G & Abdullah SS, GC-MS analysis of bioactive compounds in methanolic extracts of *Papaver decaisnei* and determination of its antioxidants and anticancer activities. *J Food Qual*, 2022 (2022) 1405157.
- 28 Ashlin ES, Edwin SG & Babila PR, Theoretical density functional analysis with experimental, electronic properties, and NBO analysis on (RS) 3-(3, 5-Dichlorophenyl) -5-methyl-5-vinylloxazolidine-2, 4-dione. *Chem Phys Impact*, 6 (2023) 100186.
- 29 Gerrit JL, Piet TVD & Ria B, Understanding Trends in Molecular Bond Angles. *J Phys Chem*, 124 (2020) 1306.
- 30 Taner E, Computational evaluation of 2-arylbenzofurans for their potential use against SARS-CoV-2: A DFT, molecular docking, molecular dynamics simulation study. *Indian J Biochem Biophys*, 59 (2022) 72.
- 31 Abduvakhid J, Utkirjon H, Hakim H, Nouredine I & Ahmad A, Intermolecular interactions in ethanol solution of OABA: Raman, FTIR, DFT, M062X, MEP, NBO, FMO, AIM, NCI, RDG analysis. *J Mol Liq*, 377 (2023) 121552.
- 32 Fathima SM & Yardily A, Synthesis, quantification, dft Calculation and molecular docking of (4-amino-2-(4-methoxyphenyl) aminothiazol-5yl) (thiophene-2yl) methanone. *Indian J Biochem Biophys*, 57 (2020) 606.
- 33 Songül S & Necmi D, Synthesis, characterization, X-ray, HOMO-LUMO, MEP, FT-IR, NLO, Hirshfeld surface, ADMET, boiled-egg model properties and molecular docking studies with human cyclophilin D (CypD) of a Schiff base compound: (E) -1-(5-nitro-2-(piperidin-1-yl) phenyl) -N-(3-nitrophenyl) methanimine. *Polyhedron*, 205 (2021) 115320.
- 34 Şükriye Ç & Taner E, Some bis (3-(4-nitrophenyl) acrylamide derivatives: Synthesis, characterization, DFT, antioxidant, antimicrobial properties, molecular docking and molecular dynamics simulation studies. *Indian J Biochem Biophys*, 60 (2023) 209.
- 35 Khadidja A, Majda SR & Michael S, DFT evaluation of structural, electronic and variation properties for complex carbohydrates with biological interest. *J Biomol Struct Dyn*, 41 (2023) 5981.
- 36 Chang GZ, Jeffrey AN & David AD, Ionization Potential, Electron Affinity, Electronegativity, Hardness, and Electron Excitation Energy: Molecular Properties from Density Functional Theory Orbital Energies. *J Phys Chem*, 107 (2003) 4184.
- 37 Reena, Biju AR, Megha PN & Bonige KB, Evaluation of antiproliferative potential of manganese (II) -dafonecomplex. *Indian J Biochem Biophys*, 58 (2021) 62.
- 38 Rahul AS, Vishnu AA, Rohit SS, Bhatu SD & Bapu SJ, Synthesis, antibacterial, antifungal and computational study of (E) -4-(3-(2, 3-dihydrobenzo[b][1, 4]dioxin-6-yl) -3-oxoprop-1-en-1-yl) benzonitrile. *Results Chem*, 4 (2022) 100553.
- 39 Moses ME, Hitler L, Emmanuel AB, Apebende GC, Obieze CE, Tomsmith OU, Asuquo BB, David P, Queen OS,

- Emmanuel IU & Tiyyati HM, Electronic structure theory study of the reactivity and structural molecular properties of halo-substituted (F, Cl, Br) and heteroatom (N, O, S) doped cyclobutane. *Phys Sci Rev*, 8 (2021) 715.
- 40 Kanagathara N, Thanigaarasu VJ, Sabari V & Elangovan S, Density Functional Theoretical Computational Studies on 3-Methyl 2-Vinyl Pyridinium Phosphate. *Adv Condens Matter Phys*, 2022 (2022) 14.
- 41 Thirunavukkarasu M, Balaji G, Muthu S, Prabakaran P & Ahmad I, Computational investigation, effects of polar and non-polar solvents on optimized structure with topological parameters (ELF, LOL, AIM, and RDG) of three glycine derivative compounds. *Struct Chem*, 33 (2022) 1295.
- 42 Vennila M, Rathikha R, Muthu S, Jeelani A & Irfan A, Theoretical structural analysis (FT-IR, FT-R), solvent effect on electronic parameters NLO, FMO, NBO, MEP, UV (IEFPCM model), Fukui function evaluation with pharmacological analysis on methyl nicotinate. *Comput Theor Chem*, 1217 (2022) 113890.
- 43 Muthukumar R, Karnan M, Elangovan N, Karunanidhi & M, Renjith T, Synthesis, spectral analysis, antibacterial activity, quantum chemical studies and supporting molecular docking of Schiff base (E) -4-((4-bromobenzylidene) amino) benzenesulfonamide. *J Indian Chem Soc*, 99 (2022) 100405.
- 44 Fathima RB, Muthu S, Johanan CP, Christina SA & Raja M, Spectroscopic (FT-IR, FT-Raman) investigation, topology (ESP, ELF, LOL) analyses, charge transfer excitation and molecular docking (dengue, HCV) studies on ribavirin. *Chem Data Collect*, 18 (2018) 250.
- 45 Jini PM, Arul DD, Hubert JI, Balachandran S & Vinitha G, Structural insights, spectral, fluorescence, Z-scan, C-H...O/N-H...O hydrogen bonding and AIM, RDG, ELF, LOL, FUKUI analysis, NLO activity of N-2(Methoxy phenyl) acetamide. *J Mol Struct*, 1272 (2023) 134140.
- 46 Janani S, Rajagopal H, Sakthivel S, Aayisha S & Raja M, Irfan A, Javed S & Muthu S, Molecular structure, electronic properties, ESP map (polar aprotic and polar protic solvents), and topology investigations on 1-(tert-Butoxycarbonyl) -3-piperidinecarboxylic acid- Anticancer therapeutic agent. *J Mol Struct*, 1268 (2022) 133696.
- 47 Sukanya R, Aruldas D, Hubert JI & Balachandran S, Spectroscopic and quantum chemical computation on molecular structure, AIM, ELF, RDG, NCI, and NLO activity of 4-VINYL benzoic acid: A DFT approach. *J Mol Struct*, 1253 (2022) 132273.
- 48 Mihaela B, Amalia S, Olga I & Oana C, Density Functional Theory (DFT) and Thermodynamics Calculations of Amino Acids with Polar Uncharged Side Chains. *Chem Proc*, 3 (2021) 08420.
- 49 Garima C & Kriti B, Quantum control of optoelectronic and thermodynamic properties of dopamine molecule in external electric field: A DFT and TD-DFT study the external electric field applied along different molecular axes. *Comput Theor Chem*, 1222 (2023) 114051.
- 50 Manju P, Muthu S & Nanje GNM, Quantum mechanical and spectroscopic (FT-IR, FT-Raman, ¹H, ¹³C NMR, UV-Vis) studies, NBO, NLO, HOMO, LUMO and Fukui function analysis of 5-Methoxy-1H-benzo[d]imidazole-2(3H) -thione by DFT studies. *J Mol Struct*, 1130 (2017) 511.
- 51 Vanasundari K, Balachandran V, Kavimani M & Narayana B, Spectroscopic investigation, vibrational assignments, Fukui functions, HOMO-LUMO, MEP and molecular docking evaluation of 4 - [(3, 4 - dichlorophenyl) amino] 2 - methylidene 4 - oxo butanoic acid by DFT method. *J Mol Struct*, 1147 (2017) 136.
- 52 Haider A, Mohd. S & AlFaify S, Density functional study of spectroscopy (IR), electronic structure, linear and nonlinear optical properties of L-proline lithium chloride and L-proline lithium bromide monohydrate: For laser applications. *Arab J Chem*, 12 (2019) 2336.
- 53 Deepa B, Natarajan C, Vignesh R & Muhammad KS, QSPR analysis of anti-asthmatic drugs using some new distance-based topological indices: A comparative study. *Int J Quantum Chem*, 124 (2024) 27372.
- 54 Jeyamangala AS, Angelin KRS, Muhammad KS & Tariq JZ, Computation of degree-based topological indices for the complex structure of ruthenium bipyridine. *Int J Quantum Chem*, 124 (2024) 27310.
- 55 Zunaira K, Shahid Z, Asad U, Muhammad KS & Melaku BB, Computation of molecular description of supramolecular Fuchisine model useful in medical data. *Sci Rep*, 10933 (2024) 14.
- 56 Shanmukha MC, Basavarajappa NS, Shilpa KC & Usha A, Degree-based topological indices on anticancer drugs with QSPR analysis. *Heliyon*, 6 (2020) e04235.
- 57 Micheal A, Ruth JKS, Shagufa M & Balasubramanian K, Relativistic topological molecular descriptors of metal trihalides. *J Mol Struct*, 1217 (2020) 128368.
- 58 Sergio B, Juan EN & Juan R, Extremal trees for the Randic index with given domination number. *Appl Math Comput*, 375 (2020) 122.
- 59 Modjtaba G & Mohammad AH, A new version of Zagreb indices. *Filomat*, 26 (2012) 93.
- 60 Xiu MZ, Yu QS, Hua W & Xiao DZ, On the ABC index of connected graphs with given degree sequences. *J Math Chem*, 56 (2018) 568.
- 61 Abeer MA, Emina M & Akbar A, General Atom-Bond Sum-Connectivity Index of Graph. *Mathematics*, 11 (2023) 494.
- 62 Yan Y, Bo Z & Nenad T, On geometric-arithmetic index. *J Math Chem*, 47 (2010) 833.
- 63 Lingping Z, The harmonic index for graphs. *Appl Math Lett*, 25 (2012) 561.
- 64 Modjtaba G & Mohammad AH, The third version of Zagreb Index. *Discrete Math Algorithms Appl*, 5 (2013) 390.
- 65 Girish VR & Usha PM, Hyper-Zagreb indices of graphs and its applications. *J Algebra Comb Discrete Appl*, 8 (2021) 9.
- 66 Guofeng Y, Muhammad KS, Mazhar H, Nazir H, Zohaib S & Fikre BP, On topological indices and entropy measures of beryllonitrene network via logarithmic regression model. *Sci Rep*, 7187 (2024) 14.
- 67 Wei G, Muhammad KS, Muhammad I, Muhammad KJ & Mohammad RF, Forgotten topological index of chemical structure in drugs. *Saudi Pharm. J*, 24 (2016) 258.
- 68 Akbar A, Suresh E & Toufik M, On the Symmetric Division Deg Index of Molecular Graphs. *MATCH Commun Math Comput Chem*, 83 (2020) 205.
- 69 Shanmukha MC, Basavarajappa NS, Shilpa KC & Usha A, Degree-based topological indices on anticancer drugs with QSPR analysis. *Heliyon*, 6 (2020) e04235.